PNAS

## Supporting Information for

# IL-11 induces NLRP3 inflammasome activation in monocytes and inflammatory cell migration to the CNS

**Maryamsadat Seyedsadr[1,2], Yan Wang[1], Manal Elzoheiry[1], Sowmya Shree Gopal[1], Soohwa Jang[1], Gayel Duran[3], Inna Chevoneva[4], Ezgi Kasimoglou[1], John Wrobel[5], Daniel Hwang[1], James Garifallou[6], Xin Zhang[7], Tabish H. Khan[8], Ulrike Lorenz[8], Maureen Su[2], Jenny P. Ting[5], Bieke Broux[3], Abdolmohamad Rostami[1], Dhanashri Miskin[1] and Silva Markovic-Plese[1]**

**Corresponding author**: Silva Markovic-Plese, TJU Department of Neurology, 900 Walnut St., Philadelphia, PA 19107, Tel: 215 503 6393, email: silva.markovic-plese@jefferson.edu

**This PDF file includes:**

Supporting text
Figures S1 to S9
Tables S1 to S2
Legends for Datasets S1 to S9
SI References

**Other supporting materials for this manuscript include the following:**

Datasets S1 to S9

## SUPPLEMENTAL MATERIALS

## EXTENDED MATERIALS AND METHODS

### Study Subjects

The human study was approved by the Thomas Jefferson University and University of Hasselt Institutional Review Board. All the subjects, 54 RRMS patients and 11 HCs signed an informed consent form prior to sample collection. The inclusion criteria for RRMS patients were RRMS diagnosis (1) and no prior treatment with DMTs, or treatment-free period for at least one year, and no prior treatment with αCD52, αVLA-4 and αCD20 mAbs. From these RRMS patients and HCs, 14 were age-, sex-, and race-matched donors of blood samples (Fig.1A). Eleven matched CSF and PBMC samples from untreated RRMS patients were used in the study (Table S1 shows demographic and disease activity markers for all subjects).

### Flow cytometry

Human blood samples were collected in heparinized tubes (BD vacutainer). PBMCs were isolated using Ficoll-Paque density gradient. Blood samples were processed in less than 18 hours. CSF cells were separated by centrifugation (400 g, 10 min) and processed the same day. For intracellular staining (ICS), cells were stimulated with PMA, Ionomycin, and Brefeldin-A (with final concentrations of 50 ng/ml, 500 ng/ml, and 3 µg/ml, respectively) for 4 hours. LPS stimulation (1 µg/ml) for 4 hours, followed by Brefeldin-A (3 µg/ml) for 2 hours was used for ICS of monocytes. Cells were stained for surface markers, fixed (Invitrogen, GAS001S), permeabilized (Invitrogen, GAS002S) and stained for intracellular markers.

For validation experiments of IL-11-induced DEGs (Fig.5), PBMCs were stimulated with IL-11 (100 ng/ml) for 48 hours in low adhesion plastic plates prior to staining.

For mice flow cytometry studies, single cell suspension was prepared from CNS, lymph nodes (LN), and spleen tissue homogenates and passed through a 70 µm cell strainer. PBMCs were isolated from blood obtained from the right atrium by Ficoll-Paque density gradient centrifugation and mononuclear cell infiltrates from CNS by 40% Percoll centrifugation gradient. Intracellular staining for NFκB, IL-1β, TLR7 and NLRP3 in validation experiments was performed following 4 hours stimulation with LPS (1 µg/ml and Brefeldin-A (3 µg/ml) for 2 hours on $LyC6^+$ gated monocytes. Data acquisition was performed on BD FACSAria Fusion flow cytometer and data analysis by FlowJo 10.6 software.

**ELISA**

To measure indicated cytokine levels, we used Human IL-23 (DY1290-05), IL-1β (DY201-05), and Mouse IL-11 (DY418) ELISA kits purchased from R&D System; Minneapolis, MD, USA) following the manufacturer's protocol. The supernatants from human monocyte cultures were incubated for 2 hours at room temperature (RT), while the mouse plasma samples were incubated overnight at RT.

**Coculture experiments**

$CD14^+$ cells were isolated from PBMCs of MS patients using the CD14 separation kit (Miltenyi Biotec). Cells were seeded in 24 well Ultra-Low Attachment Plates (Corning) and treated with or without rhIL-11 (100 ng/ml, R&D Systems) for 2 days. Monocytes were then washed and co-

cultured with separated autologous $CD4^+$ cells at 1:1 ratio. After 24 hours, cells were harvested and the expression of cytokines was assessed in gated $CD4^+$ cells.

**Migration assay**

Human cerebral microvascular endothelial cells (hCMEC/d3) were provided by Tebu-bio (le Perray-en-Yevelines, France) and were seeded at 1-1.2×$10^6$ cells/$cm^2$ onto coated plates or inserts with 75 µg/mL rat tail collagen type I solution (Merck). Cells were grown in EGM™-2MV Microvascular Endothelial Cell Growth Medium-2 BulletKit™ (CC-3202, Lonza) with 2.5% fetal bovine serum (FBS) (Gibco™, Thermo Fisher Scientific) up to 80-90 % confluency. For migration assays, hCMEC/d3 cells were cultured in collagen coated Thincerts (24 well, translucent, 3 µm, Greiner Bio-One, Vilvoorde, Belgium) at a density of 25x$10^3$ cells/$cm^2$. Three and five days after seeding the cells, medium was replenished and supplemented with 5 ng/ml human fibroblast growth factor (hFGF), 1.4 µM hydrocortisone, 10 mg/ml gentamicin, 1 mg/ml amphotericin (A2942, all Merck) and 2.5% FCS). After reaching confluence on day six hCMEC/d3 cells were replenished with serum reduced experimental medium (EMB™-2 Basal Medium, 5 ng/ml hFGF, 10 mg/ml gentamicin, 1 mg/ml amphotericin and 0.25% FCS) and treated with TNFα (100 ng/ml) and IFN-γ (10 ng/ml) for 24 hours. PBMCs were isolated from 3 HCs and cultured 2x$10^6$/ml in RPMI supplemented with 10% FCS, 1%NEAA, 1% NaPyr and 0.5% Pen/strep. Cells were either left untreated, treated with IL-11 (R&D systems, 100 ng/ml) or IL-11 (100 ng/ml) with αIL-11 mAb (Biolegend, 10 µg/ml) for 24 hours. The inserts were washed with PBS, and PBMCs were added (3.7-3.9x$10^5$ per insert, 3 inserts per condition). PBMCs migrated for 24 hours. Cells from the well (migrated) were collected, counted using an automatic cell counter (Moxi–Orflo technologies, Ketchum, US), and phenotyped using flow cytometry.

Cells were stained with viability dye (eF506, fixable viability dye (FVD) Invitrogen), CD16 (FITC), CD14 (BV605), CD8 (BV711), CD19 (BV785), HLA-DR (AF700), CD4 (APC-Fire750) mAb, all from Biolegend, and IL-11R mAb (AF594, SantaCruz).

Mice migration experiments were performed using magnetic bead-separated $Ly6C^+$ monocytes from bone marrow of C57BL/6 mice, treated with rm IL-11 in the absence or presence of αIL-11 mAb (MAB418) for 24 hours ($0.5x10^6$ cells per condition). Cells were washed and transferred to the upper chamber of Transwell with 5 µm pore size in 100 µl of medium and allowed to migrate for 12 hours. Unmigrated cells were removed from the upper chamber, inserts were fixed, and stained with Dapi. Using Zeiss Observer Z1 microscope, the migrated monocytes attached to the insert were enumerated in 10 different microscopic fields using 10x magnification and quantified using ImageJ software.

**Single cell RNA sequencing**

Blood samples from three recently diagnosed untreated RRMS patients were lysed with RBC lysis buffer (eBioscience) following manufacturer's instructions. Cells stained for IL-11R and sorted using FACS Aria fusion were stimulated with 100 ng/ml rh IL-11 (R&D Systems) for 1 hour or kept unstimulated. CSF and blood samples from two RRMS patients were sorted for $IL\text{-}11R^+$ cells following RBC lysis for blood samples. In order to decrease batch-to-batch variations, all samples from each experiment were submitted for scRNAseq on the same day. Next-generation sequencing libraries were prepared using the 10x Genomics Chromium Single Cell 3' Reagent kit v3 as per manufacturer's instructions. Library quality control was assessed using Agilent TapeStation for sizing (bp) and KAPA qPCR for concentration. Libraries were uniquely indexed using the Chromium i7 Sample Index Kit, pooled, and sequenced on the

Illumina NovaSeq6000 sequencer in a paired-end, single indexing run. Sequencing depth targeted 20000 mean reads per cell. Data were then processed using the Cellranger pipeline (10x genomics, v.5.0.0) for demultiplexing and alignment of sequencing reads to the GRCh38 transcriptome and creation of feature-barcode matrices. Individual single cell RNAseq libraries were aggregated using the Cellranger pipeline. Libraries were normalized for sequencing depth across all libraries during aggregation. Secondary analysis on the aggregated feature barcode matrix was performed using the Seurat package (v.4.0) within the R computing environment. Briefly, cells expressing less than 200 or more than 5000 genes were excluded from the analysis. Additionally, cells expressing >25% mitochondrial genes were excluded from the dataset. The data were normalized by multiplying the expression by a factor of 10,000 and performing log transformation of the result (Seurat v4) (2). Variable features across single cells in the dataset were identified by mean expression and dispersion, and expression data was scaled across all genes in the dataset. Identified variable features were used to perform a principal component analysis (PCA). The dimensionally-reduced data were used to cluster cells and visualize them using a UMAP plot (dimensions 1:20, resolution 0.5).

Annotation was performed for the main immune cell subsets and sub-classification with the SingleR package based on the published data available (3). Briefly, singleR uses the gene expression signatures to calculate a spearman correlation coefficient for every cell. To assign cells within the dataset, the top scoring cell type was utilized. Differential expression (DE) and marker gene detection was performed using the FindMarkers and FindAllMarkers functions in the Seurat R package with the default Wilcoxon Ranked Sum test. Genes were considered differentially expressed if they had an average log fold-change of at least 0.25 and a Bonferroni-adjusted p value of 0.05 or lower (volcano plots). For DE including all cells of the 10x dataset, a

minimum of 10% of cells had to express the gene and at least 10 cells had to express the gene in each group. Violin plots show the expression level of the selected significantly up-regulated genes.

Upregulated genes in IL-11 stimulated/unstimulated or CSF/blood samples identified with R (adjusted p-value<0.05, and log2 fold change >0.25) were used for Gene Ontology (GO). KEGG pathway analysis and biological processes was performed using DAVID Bioinformatics Resources 6.8. Significant pathways and Biological processes were provided in the figures based on their significance and biological relevance.

**Quantitative Real-Time PCR (qRT-PCR)**

For the RRMS patients, both $CD4^+$ T cells and monocytes were separated using Stem cell isolation kits (EasySepRelease Human CD4 Positive Selection Kit # 17752 and EasySep Human Monocyte Isolation Kit# 19359, respectively). Isolated cells were stimulated with 100 ng/ml rhIL-11 for 6 hours, followed by RNA extraction (Zymo Research), cDNA generation (Invitrogen) and gene expression measurements using Taqman probes (Table S2). qRT-PCR was performed using Quantstudio 3 in triplicate and results are expressed as a relative expression normalized to GAPDH.

For mice, IL-$11R^+$ monocytes were separated (EasySep Mouse Monocyte Isolation Kit #19861 then EasySep PE Positive Selection Kit II #17684, StemCell technologies) from spleen of mice with RREAE and stimulated with 100 ng/ml rmIL-11 for 9 hours. From mice treated with αIL-11 mAb or control isotype, IL-$11R^+$ monocytes were separated, followed by RNA extraction (Zymogen Research) and cDNA generation (Invitrogen) for qRTP-CR using Quantstudio 3 in triplicate. The results are expressed as a relative expression normalized to β actin.

**Western blotting**

Monocytes were separated using magnetic beads (StemCell technologies # 19861) from Bl6 mice spleen cells, and $10^6$ cells per condition were incubated in the absence or presence of rm IL-11 (R&D Systems # 418-ML) dose titration and αIL-11 mAb (10 μg/ml, (R&D Systems # MAB418) for 30 min. Cell lysates were denatured in SDS and resolved by 10% SDS-PAGE then transferred to PVDF membranes (Millipore # IPVH00010). The membranes were probed with primary Abs against mouse total and phosphorylated STAT3, ERK1/2, NFκB p65, and β-actin overnight at 4°C, followed by HRP-conjugated IgG secondary Ab (Santa Cruz Biotechnology) incubation for 1 hour at RT. Membranes were developed using West Pico PLUS Chemiluminescent Substrate (ThermoFisher # 34580) then imaged using the iBright 1500 imaging system.

**EAE**

Active RREAE was induced in female SJL mice (8-10 weeks old, purchased from the Jackson Laboratory) with $PLP_{139-151}$ peptide. Briefly, mice were injected with the immunization emulsion containing 1:1 ratio of *M. tuberculosis* in incomplete Freund's adjuvant (8 mg/ml) and 60 μg/mouse $PLP_{139-151}$ peptide (Anaspec, AS-63912). 200 ng pertussis toxin (List Biological Laboratories #180) was injected intraperitoneally (i.p.) on days 0 and 2. Clinical scores were recorded daily: 1) limp tail, 2) hind limb weakness, 3) hind limb paralysis, 4) hind limb paralysis and forelimb weakness and 5) moribund mice. Clinical scores are presented as mean ± SEM. Daily i.p injections of anti-mouse IL-11 mAb (15 mg/kg, MAB418, R&D systems) or isotype

control IgG2 mAb (R&D systems) were administered starting at the onset of clinical disease for 10 consecutive days; onset=10 d.p.i,. peak=14 d.p.i., remission=22 d.p.i.

**Immunohistofluorescence**

At 18 days post immunization, mice were anesthetized and perfused with PBS and then by 4% paraformaldehyde. The spinal columns were fixed in 4% PFA overnight and spinal cord dissected the next day. After cryopreservation with sucrose 30%, spinal cords were cut in cervical, thoracic, lumbar, and sacral segments and embedded in OCT medium (Fischer Scientific). The frozen blocks were prepared by placing the embedding molds in ethanol cooled by dry ice. 10 μm sections were cut from spinal cords and collected on superfrost/Plus slides (Fischer Scientific). Immunostaining was performed as previously described (4). Slides were incubated with primary antibodies overnight at 4°C; the next day slides were washed and secondary antibodies were applied for 1 hour. Slides were mounted with ProLong™ Diamond Antifade Mountant with DAPI (Invitrogen). The antibodies used for immunofluorescence study are listed in Table S2. H&E staining was used to quantify the number of inflammatory foci (defined as 10 nuclear cells) by a blinded investigator (5). Demyelinated area was identified by lack of MBP staining in 8 spinal cord sections. Immunostaining for CD4, IL-11 and Iba-1 was quantified in at least 8 fields (635 $\mu m^2$) in the lesion. Quantification was performed using Nikon A1R microscope and Image J software. The results are presented as mean demyelination area ($mm^2$) (n=5 mice per group, scale bar=200 μm).

**Statistical analysis**

For data reported in Fig. 1A, we used Kruskal-Wallis test with Dunn's post-test adjustment for multiple comparisons to determine the differences in frequency of IL-11$^+$ and IL-11RA$^+$ cells among 7 PBMC cell subsets. All marker comparisons between the IL-11$^+$ and IL-11RA$^+$ cells reported in Fig. 1B and C were performed using nonparametric two-sample Mann-Whitney/Wilcoxon rank-sum test, with Benjamini test for the false discovery rate. Data are presented as Mean ± SEM; *p<0.05, **p<0.01, *** p<0.001.

The differences between marker expressions in PBMC and CSF cells from the same patient (reported in Fig. 2) were evaluated using non-parametric Wilcoxon matched pairs test with Benjamini post-test adjustment. *p<0.05, **p<0.01.

ScRNAseq data were analyzed using Wilcoxon Rank Sum test (FindMarkers and FindAllMarkers functions in the Seurat R package) followed by Bonferroni's post-test. The genes with Bonferroni-adjusted p-value<0.05 and log2 FC>0.25 or <-0.25 are considered differentially expressed. Data were visualized by the violin plots, whisker plots with median expression. Pathway analysis and Gene ontology data were analyzed by Fisher's exact test followed by Benjamini-Hochberg post-test as built in functions in DAVID software.

The differences between marker expressions (obtained using qRT-PCR and flow cytometry) in IL-11-stimulated and non-stimulated cells (Fig. 5) from the same patient samples were compared using non-parametric paired Wilcoxon test. Data in Fig. 6 were tested for normal distribution using Shapiro-Wilk test. Based on the distribution, data were analyzed using non-parametric Kruskal-Wallis test for multiple groups (Fig. 6A), Wilcoxon matched-paired test for two groups with matched samples (Fig 6B) or Mann-Whitney/Wilcoxon rank-sum test for two groups with independent samples (Fig. 6D-K, M). Where data distribution was normal, we used paired (Fig. 6L) or unpaired t-test (Fig. 6C).

Statistical analysis was performed using GraphPad Prism 9 and R version 4.2.2. In all reports * indicates $p<0.05$, **$p<0.01$, ***$p<0.005$.

**Study approval**

All subjects signed an informed consent form prior to sample collection. Animal experiments were conducted following the approval of the Institutional Animal Care and Use Committee (IACUC) of Thomas Jefferson University and UCLA.

**Fig. S1.**

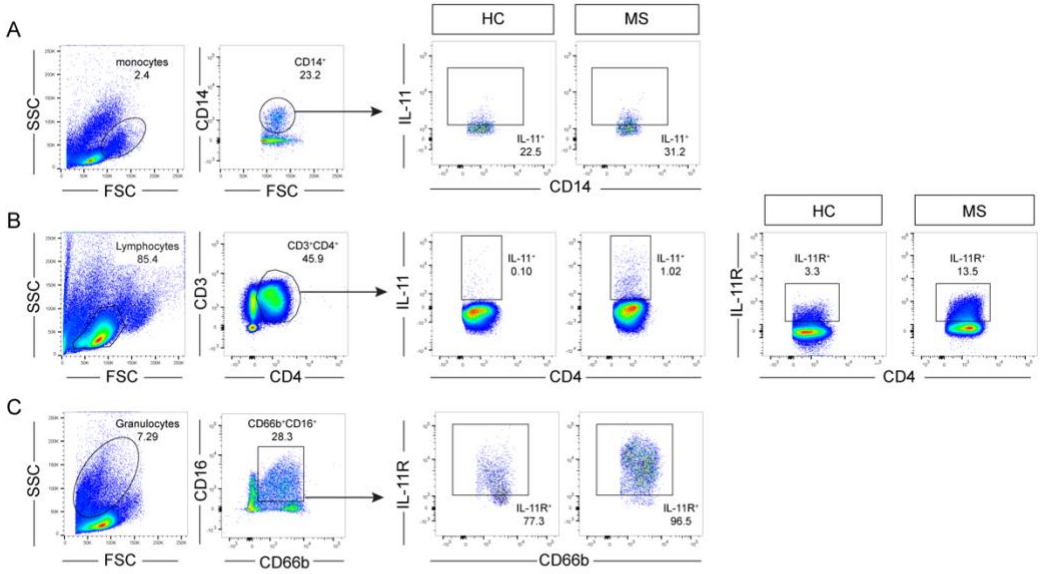


**Figure S1.** Representative flow cytometry staining for IL-11$^+$CD14$^+$ monocytes, IL-11$^+$ and IL-11R$^+$ CD4$^+$ T cells and IL-11R$^+$CD16$^+$CD66$^+$ neutrophils, which have increased frequency in RRMS patients. FACS gating strategy for quantification of IL-11$^+$ cells in CD14$^+$ monocytes; IL-11$^+$ and IL-11R$^+$ CD3$^+$CD4$^+$ cells; and IL-11$^+$ cells in CD16$^+$CD66$^+$ neutrophils in HCs and RRMS patients.

**Fig. S2.**

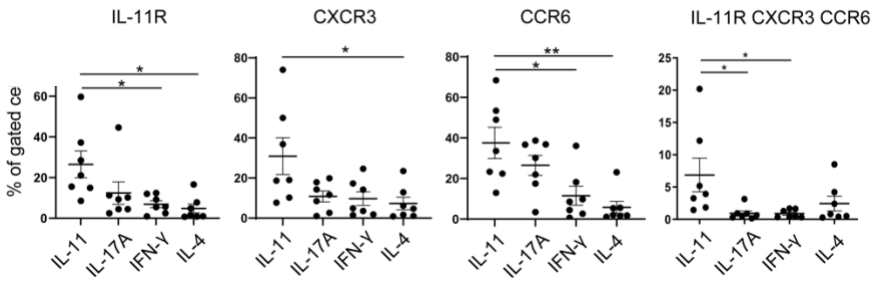


**Figure S2.** Phenotype of IL-11$^{+}$CD4$^{+}$ cells in comparison to Th1, Th1 and Th2 cells. Frequency of IL-11R$^{+}$, CCR6$^{+}$ and CXCR3$^{+}$ cells in IL-11$^{+}$, Th17 (IL-17A$^{+}$), Th1 (IFN-γ$^{+}$), and Th2 (IL-4$^{+}$) CD4$^{+}$ T cells from RRMS patients (n=7, one-way ANOVA with Bonferroni multiple comparison post-test).

**Fig. S3**

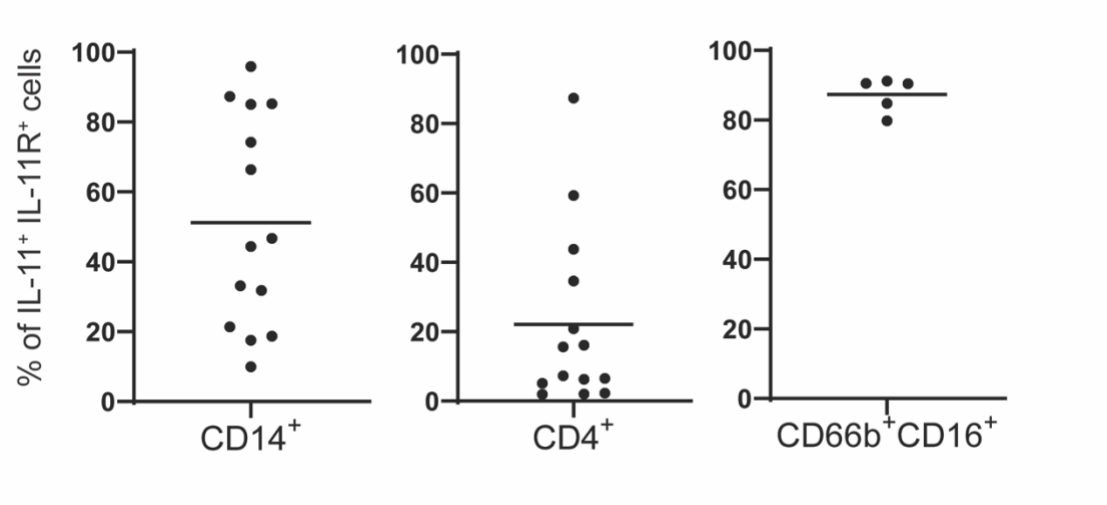


**Figure S3.** Co-expression of IL-11 and IL-11R in monocytes, $CD4^+$ cells, and neutrophils (n=14 for $CD14^+$ and $CD4^+$, n=5 for $CD66b^+CD16^+$ cells).

**Fig.S4.**

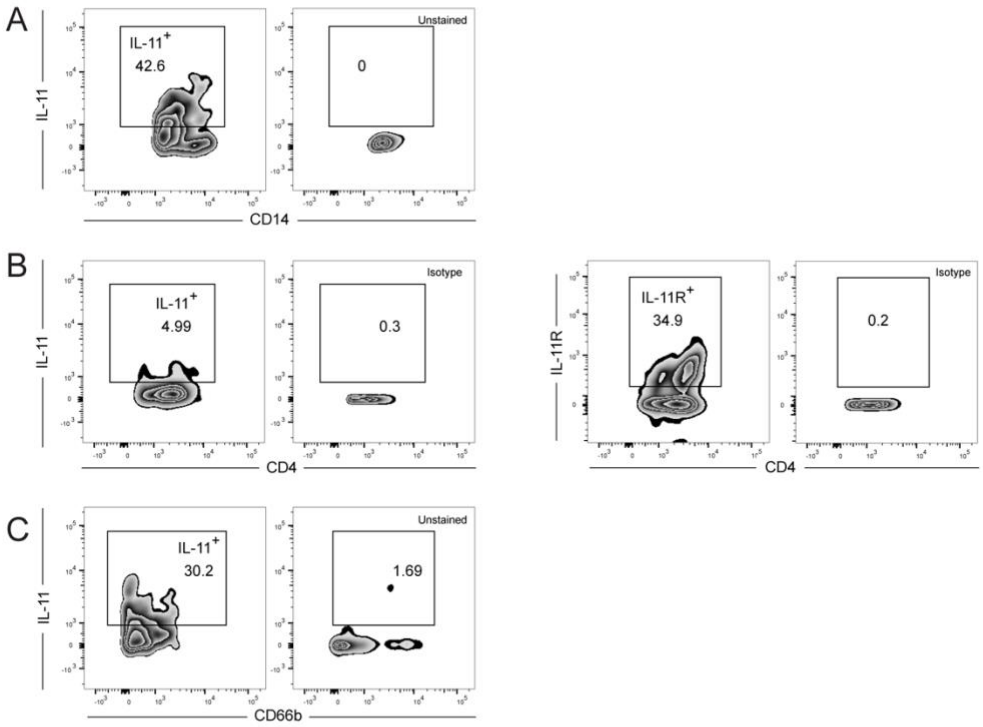


**Figure S4.** Representative staining of IL-11$^{+}$ monocytes, IL-11$^{+}$ and IL11R$^{+}$ CD4$^{+}$ T cells and IL-11$^{+}$ neutrophils accumulated in CSF of RRMS patients**.** **A**) Representative staining for IL-11$^{+}$ cells in CD14$^{+}$ monocytes; **B**), IL-11$^{+}$ and IL-11R$^{+}$ cells in CD3$^{+}$CD4$^{+}$ cells and **C)** IL-11$^{+}$ CD16$^{+}$CD66$^{+}$ neutrophils, accumulated in the CSF of RRMS patients.

**Fig. S5.**

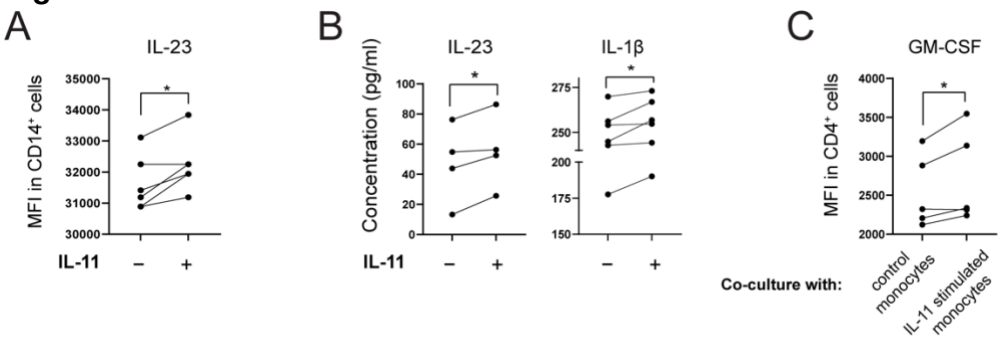


**Figure S5**. IL-11$^+$ monocytes have inflammatory phenotype. **A**) Magnetic bead-separated CD14$^+$ cells from RRMS patients were treated with LPS (with or without rhIL-11 (100 ng/ml) for 48 h, and the expression of intracellular cytokines was measured by mean fluorescence intensity (MFI) (n=6, paired t-test). **B**) Supernatants from unstimulated and IL-11-stimulated CD14$^+$ cells were used for ELISA cytokine measurements (n=4 and 6, paired t-test). **C**) Magnetic bead-separated CD14$^+$ cells from RRMS patients were stimulated with or without rhIL-11 for 48 h, washed, and co-cultured with separated CD4$^+$ cells from the same donor. Cytokine expression in CD4$^+$ cells was tested by flow cytometry (n=5, paired t-test).

**Fig. S6.**

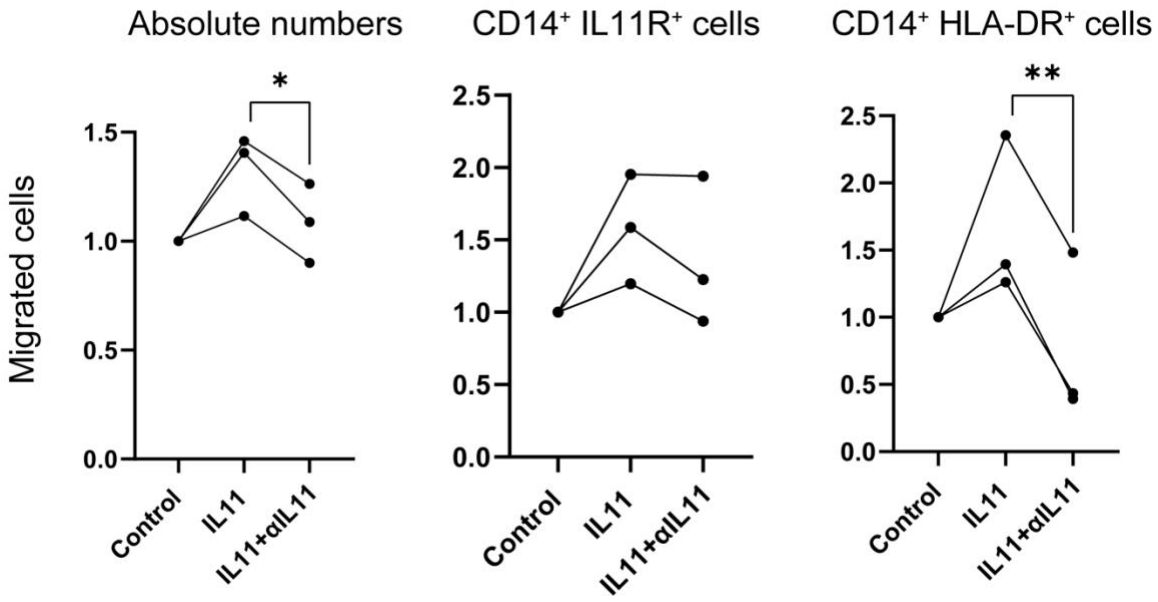


**Figure S6.** IL-11 induces IL-11R$^+$ and HLA-DR$^+$ monocytes migration across the human cerebral vascular endothelial cell barrier. PBMCs from 3 HCs were added to the human endothelial cell (hCMEC/d3) covered inserts, and allowed to migrate for 24 h. Cells that migrated were counted and stained for indicated markers by flow cytometry. The absolute number of cells that migrated following IL-11 stimulation were normalized against the unstimulated condition. The mean fluorescence intensity (MFI) of IL-11R and HLA-DR expression on migrated monocytes were normalized to the MFI of IL-11R and HLA-DR expressed on the control cells. Statistical analysis was performed using one way ANOVA with Dunnet multiple comparison correction *$p<0.05$, **$p<0.01$.

**Fig. S7.**

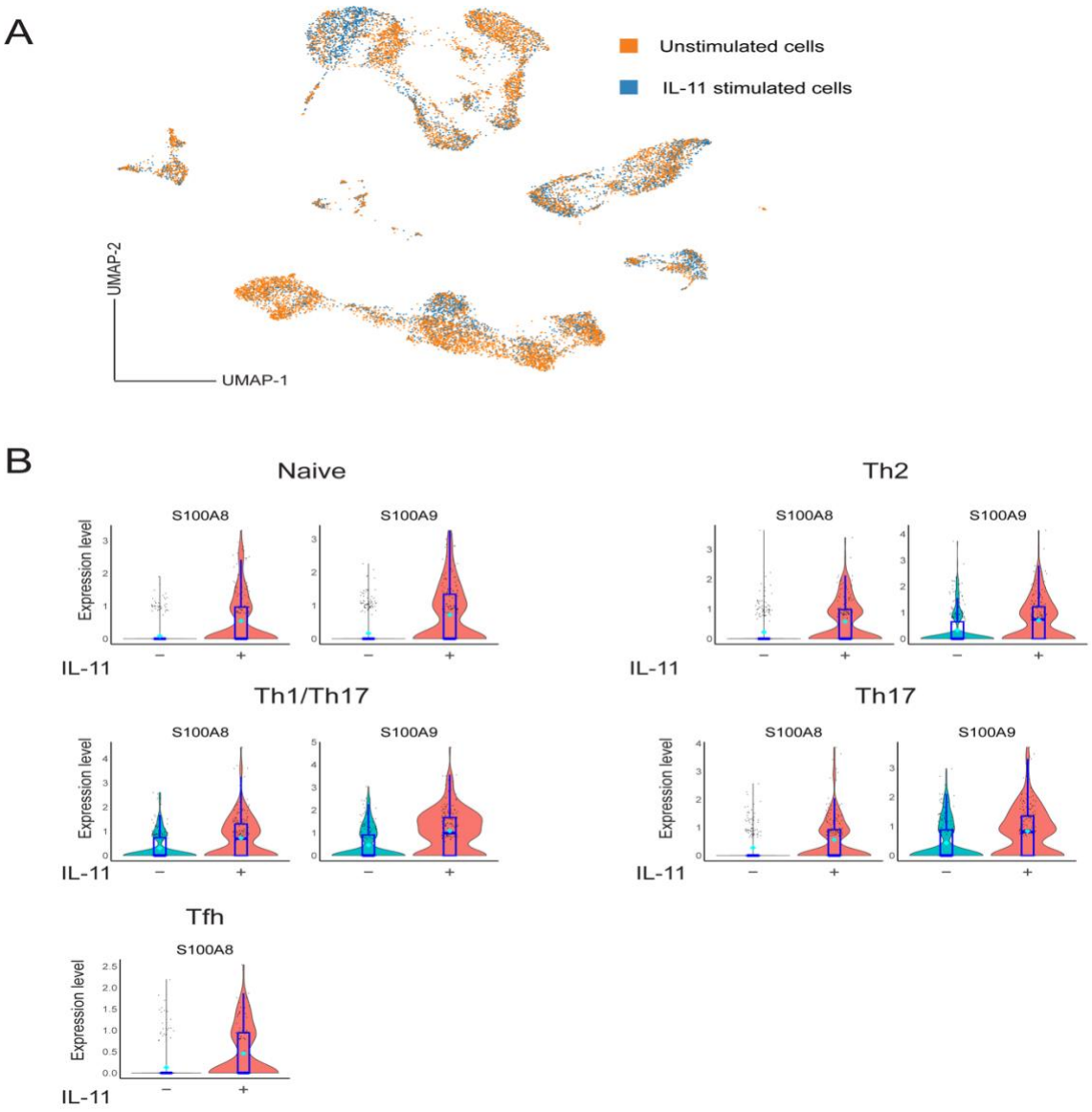


**Figure S7.** Single cell RNA sequencing of IL-11 stimulated vs. unstimulated IL-11R$^{+}$ sorted cells from RRMS patients. **A)** The UMAP projection for IL-11-stimulated and unstimulated cells. The UMAP presents clustering of 6,478 IL-11-stimulated and 8,368 unstimulated cells, please see annotation of 29 immune cell types in Fig. 3B. **B)** Violin plots present significantly increased S100A8 and S100A9 gene expression in IL-11 stimulated CD4$^{+}$ T cell subsets.

**Fig S8.**

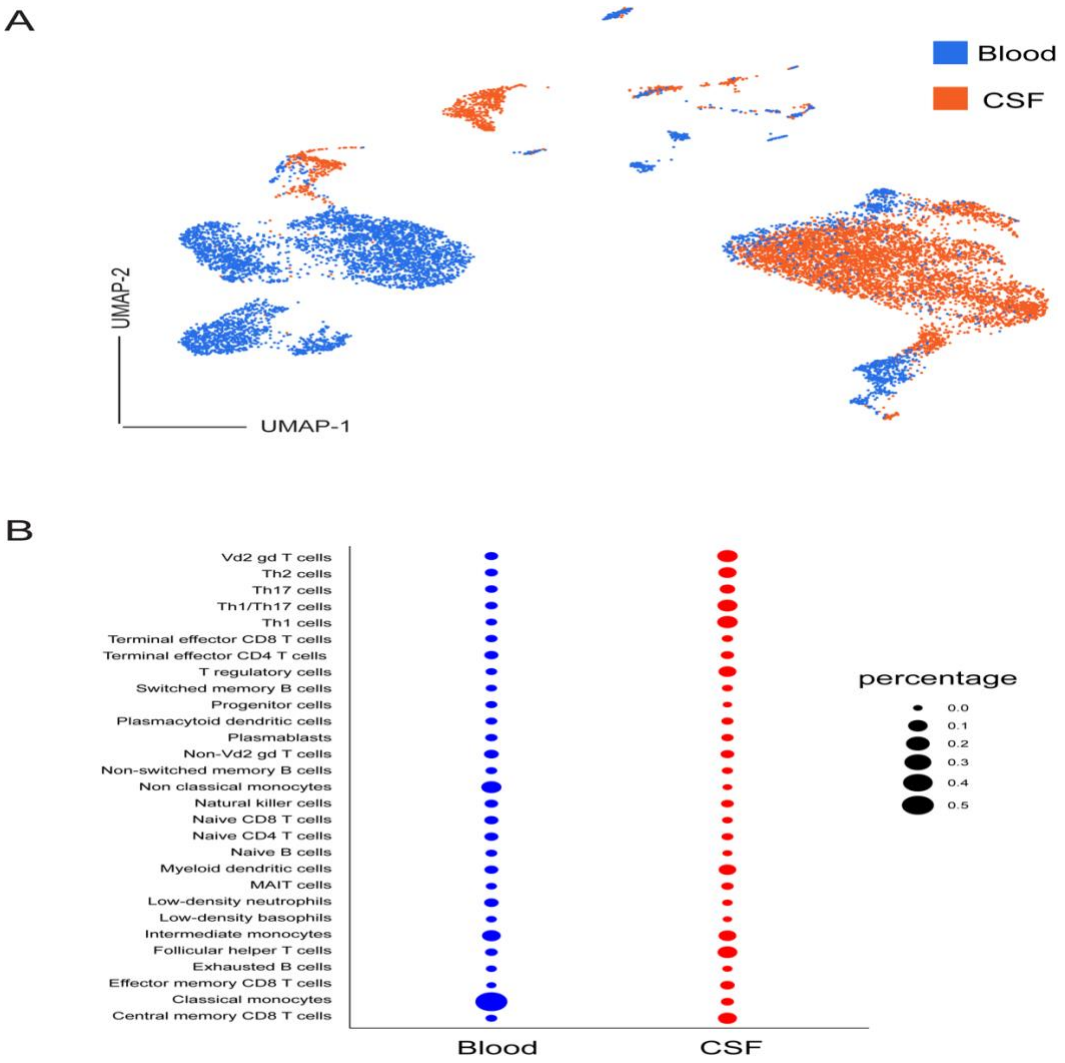


**Figure S8**. scRNAseq of IL-11R$^{+}$ sorted cells from blood and CSF of RRMS patients. **A**) The UMAP projection for CSF and blood IL-11R$^{+}$ sorted cells. The UMAP presents clustering of 6,609 CSF and 5,772 blood-derived IL-11R$^{+}$ sorted cells from 2 RRMS patients, please see annotation of 29 immune cell types in Fig. 4A. **B**) A comparison of the abundance of each cell type in CSF and blood (the percentage of each cell subset from the total cell number in each compartment), Dataset S7.

**Fig.S9.**

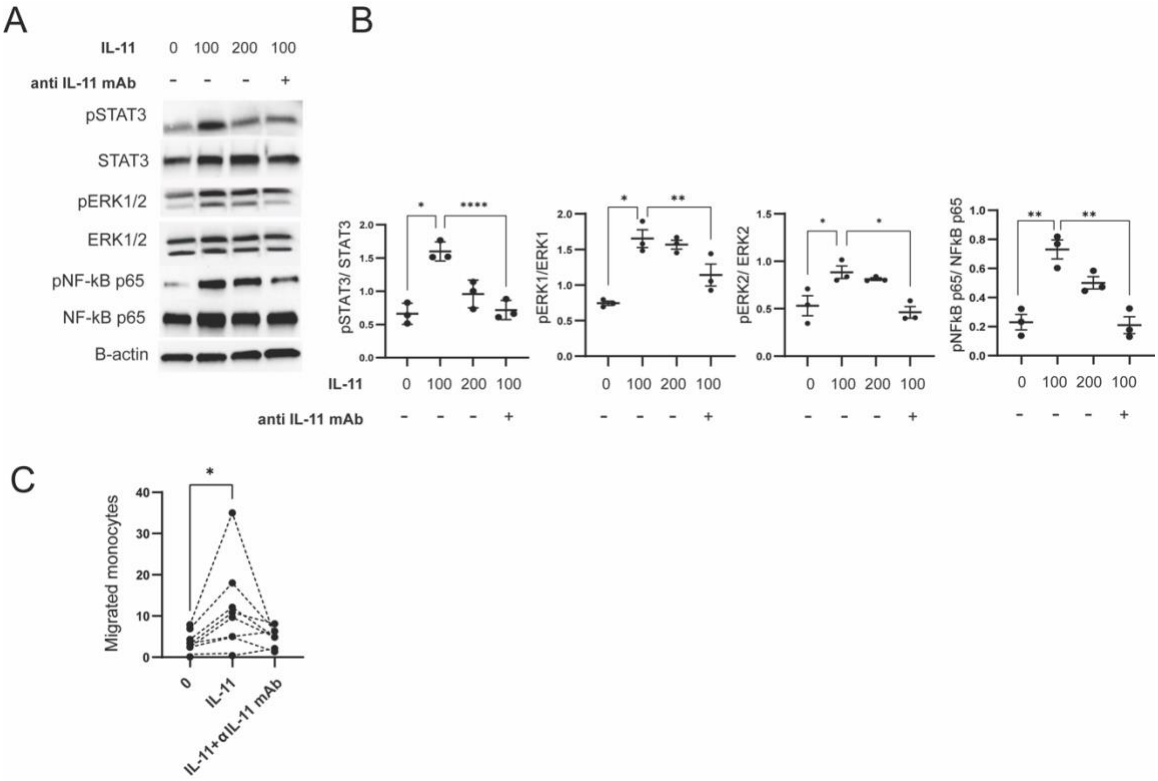


**Figure S9. A)** αIL-11 mAb inhibits IL-11-induced mouse monocyte activation. $CD11b^{+}Ly6C^{+}$ monocytes were separated from C57/Bl6 mice spleen using magnetic beads and incubated with rmIL-11 (100 ng/ml) in the absence or presence of m αIL-11 mAb (10 μg/ml). Total and phosphorylated STAT3, ERK1/2 and p65 NFκB were determined by WB after 30 min. **B)** Protein quantification was done by normalizing pSTAT3, pERK1/2 and pNFκB p65 against the total protein, β-actin was used as a loading control. Normalized data are presented as mean ± SD of three independent experiments. Statistical analysis was performed using one-way ANOVA with Tukey post hoc test; *p<0.05, **p<0.01, *** p<0.005. **C**) $0.5x10^{6}$ monocytes per condition were cultured with rm IL-11 in the absence or presence of m αIL-11 mAb for 24 h. Cells were loaded in the upper chamber of the transwell and allowed to migrate for 12 h. Migrated cells attached to the insert were fixed, stained and counted in 10 different 10x fields in each condition.

**Table S1.** Demographic and disease activity data for study subjects.

| Subject | Age | Sex | Race | Disease duration (month) | EDSS | Figures in paper | Matched HC subject |
|---|---|---|---|---|---|---|---|
| MS1 | 54 | Female | Caucasian | 1 | 6 | Fig1 A/B/C, S Fig 2, S Fig 3 | HC1 |
| MS2 | 49 | Female | Caucasian | 1 | 1 | Fig1 A/B/C, S Fig 2, S Fig 3 | HC10 |
| MS3 | 49 | Female | Caucasian | 2 | 2.5 | Fig1 A/B/C, S Fig 2, S Fig 3 | HC8 |
| MS4 | 35 | Female | Caucasian | 1 | 6 | Fig1 A/B/C, S Fig 2, S Fig 3 | HC5 |
| MS5 | 24 | Female | Caucasian | 1 | 0 | Fig1 A/B/C, S Fig 2, S Fig 3 | HC3 |
| MS6 | 35 | Male | Caucasian | 1 | 2.5 | Fig1 A/B/C, S Fig 2, S Fig 3 | HC4 |
| MS7 | 42 | Female | African-American | 1 | 6 | Fig1 A/B/C, S Fig 2, S Fig 3 | HC7 |
| MS8 | 53 | Female | Caucasian | 1 | 1 | Fig1 A/B/C, S Fig 2, S Fig 3 | HC6 |
| MS9 | 24 | Female | Caucasian | 1 | 6 | Fig1 A/B/C, S Fig 2, S Fig 3 | HC2 |
| MS10 | 20 | Female | African-American | 2 | 0 | S Fig 2 | - |
| MS11 | 45 | Female | Caucasian | 180 | 0 | S Fig 2 | - |
| MS12 | 55 | Female | Caucasian | 24 | 1 | Fig1 A/B/C, S Fig 2, S Fig 3 | HC9 |
| MS13 | 26 | Female | Caucasian | 1 | 3.5 | Fig1 A/B/C, S Fig 2, S Fig 3 | HC11 |
| MS14 | 53 | Male | Caucasian | 1 | 1 | S Fig 2 | - |
| MS15 | 39 | Female | African-American | 2 | 3.5 | Fig1 A/B/C, S Fig 2, S Fig 3 | HC12 |
| MS16 | 34 | Female | African-American | 48 | 0 | Fig1 A/B/C, S Fig 2, S Fig 3 | HC14 |
| MS17 | 45 | Female | African-American | 72 | 0 | S Fig 2 | - |
| MS18 | 23 | Female | African-American | 4 | 3.5 | Fig1 A/B/C, S Fig 2, S Fig 3 | HC13 |
| MS19 | 26 | Female | African-American | 2 | 0 | S Fig 2 | - |
| MS20 | 23 | Female | Caucasian | 1 | 2 | Fig 2 | - |
| MS21 | 57 | Male | Caucasian | 1 | 1.5 | S Fig 5 | - |
| MS22 | 32 | Female | Caucasian | 3 | 1 | Fig 2, S Fig 5 | - |
| MS23 | 42 | Female | Caucasian | 1 | 1 | S Fig 5 | - |
| MS24 | 52 | Female | African-American | 3 | 1 | S Fig 5 | - |
| MS25 | 45 | Female | African-American | 72 | 0 | Fig 3, S Fig 5 | - |
| MS26 | 32 | Female | Caucasian | 11 | 0 | S Fig 5 | - |

| | | | | | | | |
|---|---|---|---|---|---|---|---|
| MS27 | 39 | Female | African-American | 24 | 4 | S Fig 5 | - |
| MS28 | 54 | Male | Caucasian | 8 | 1 | S Fig 5 | - |
| MS29 | 36 | Female | African-American | 1 | 6 | S Fig 5 | - |
| MS30 | 55 | Female | African-American | 1 | 5 | Fig 2, Fig 3, S Fig 5 | - |
| MS31 | 49 | Female | African-American | 6 | 0 | Fig 3 | - |
| MS32 | 27 | Female | African-American | 16 | 1 | Fig 5 | - |
| MS33 | 53 | Male | African-American | 1 | 2 | Fig 5 | - |
| MS34 | 29 | Female | African-American | 6 | 1 | Fig 5 | - |
| MS35 | 37 | Female | Caucasian | 4 | 1.5 | Fig 5 | - |
| MS36 | 32 | Female | African-American | 120 | 2.5 | Fig 5 | - |
| MS37 | 63 | Female | African-American | 120 | 6.5 | Fig 5 | - |
| MS38 | 40 | Female | African-American | 4 | 0 | Fig 5 | - |
| MS39 | 45 | Female | African-American | 120 | 0 | Fig 5 | - |
| MS40 | 47 | Female | African-American | 24 | 3 | Fig 5 | - |
| MS41 | 43 | Female | Caucasian | 2 | 2 | Fig 5 | - |
| MS42 | 33 | Male | Caucasian | 3 | 1 | Fig 5 | - |
| MS43 | 29 | Female | Caucasian | 48 | 2 | Fig 5 | - |
| MS CSF1 | 23 | Female | Caucasian | 2 | 1 | Fig 2 | |
| MS CSF2 | 32 | Female | Caucasian | 1 | 3 | Fig 2 | |
| MS CSF3 | 55 | Female | African-American | 1 | 4.5 | Fig 4 | |
| MS CSF4 | 48 | Female | African-American | 5 | 1.5 | Fig 2 | |
| MS CSF5 | 25 | Female | Caucasian | 1 | 2 | Fig 2 | |
| MS CSF6 | 44 | Male | Caucasian | 1 | 2 | Fig 2 | |
| MS CSF7 | 55 | Female | African-American | 2 | 5 | Fig 4 | |
| MS CSF8 | 51 | Male | Caucasian | 1 | 1 | Fig 2 | |
| MS CSF9 | 27 | Female | Caucasian | 1 | 4 | Fig 2 | |
| MS CSF10 | 58 | Male | Caucasian | 4 | 2 | Fig 2 | |
| MS CSF11 | 31 | Male | Caucasian | 3 | 0 | Fig 2 | |
| Average | 39.8 | F/M=44/10 | AA/Caucas=/24/30 | 18 | 2.1 | | |
| HC1 | 55 | Female | Caucasian | | | Fig 1 B/C | MS1 |
| HC2 | 24 | Female | Caucasian | | | Fig 1 B/C | MS9 |

| | | | | | | | |
|---|---|---|---|---|---|---|---|
| HC3 | 24 | Female | Caucasian | | | Fig 1 B/C | MS5 |
| HC4 | 35 | Male | Caucasian | | | Fig1 B/C | MS6 |
| HC5 | 35 | Female | Caucasian | | | Fig1 B/C | MS4 |
| HC6 | 53 | Female | Caucasian | | | Fig 1 B/C | MS8 |
| HC7 | 42 | Female | African-American | | | Fig 1 B/C | MS7 |
| HC8 | 47 | Female | Caucasian | | | Fig 1 B/C | MS3 |
| HC9 | 55 | Female | Caucasian | | | Fig 1 B/C | MS12 |
| HC10 | 48 | Female | Caucasian | | | Fig 1 B/C | MS2 |
| HC11 | 25 | Female | Caucasian | | | Fig 1 B/C | MS13 |
| HC12 | 39 | Female | African-American | | | Fig 1 B/C | MS15 |
| HC13 | 23 | Female | African-American | | | Fig 1 B/C | MS18 |
| HC14 | 34 | Female | Caucasian | | | Fig 1 B/C | MS16 |
| HC15 | 29 | Female | Caucasian | | | S Fig 6 | - |
| HC16 | 26 | Female | Caucasian | | | S Fig 6 | - |
| HC17 | 43 | Female | Caucasian | | | S Fig 6 | - |
| Average | 37.5 | F/M=16/1 | AA/Caucas=3/14 | | | | |

**Table S1.** Demographic data for blood and CSF RRMS patient donors and HCs. EDSS, Expanded Disability Status Scale is a RRMS disease-related disability measure.

**Table S2. Reagents used in the study**

| antibodies for humans | | | | |
|---|---|---|---|---|
| Antigen | Fluorochrome | Clone | Supplier | Identifier |
| CD3 | PE-Cy5.5 | SK7 | Invitrogen | 35-0036-42 |
| CD4 | BV786 | SK3 | BD Bioscience | 563877 |
| CD8 | BV605 | SK1 | BioLegend | 344742 |
| CD19 | AF700 | HIB19 | BioLegend | 302226 |
| CD56 | BV605 | 5.1 H11 | BioLegend | 362538 |
| CD11c | BV510 | B-ly6 | BD Bioscience | 563026 |
| CD14 | AF700 | 63D3 | BioLegend | 367114 |
| CD66 | AF700 | VI MA81 | BioLegend | 305114 |
| CD25 | BV510 | M-A251 | BD Bioscience | 563352 |
| IL-11RA | AF647, FITC, PE | 4D12 | Santa Cruz | sc-130920 |
| VLA4 (CD49d) | FITC | 9F10 | BD Bioscience | 560840 |
| CCR6 (CD196) | BV650 | 11A9 | BD Bioscience | 563922 |
| ICAM-1 (CD54) | PE-Cy5 | HA58 | BD Bioscience | 555512 |
| CXCR3 (CD183) | BV605 | G025H | BioLegend | 353728 |
| CCR2 (CD192) | BV510 | LS132.1D9 | BD Bioscience | 747851 |
| IL-11 | PE | 22626 | R&D Systems | MAB218 (custom labeled PE) |
| IFN-γ | BV711 | B27 | BD Bioscience | 564039 |
| GM-CSF | PE-CF594, PerCpCy5.5 | BVD2-21C11 | BD Bioscience | 562857, 502312 |
| IL-17A | PerCpCy5.5 BV421 | N49-653 | BD Bioscience | 560799 562933 |
| IL-4 | PE-Cy7 | 8D4-8, | BD Bioscience | 560672 |
| IL-10 | PE-CF594 | JES3-19F1 | BD Bioscience | 562400 |
| IL-23 | FITC | C-3 | SANTA CRUZ | Sc-271279 |
| FoxP3 | PE-CF594 | 236A/E7 | BD Bioscience | 563955 |
| T-bet | FITC | 4B10 | BioLegend | 644812 |
| RORγt | BV650 | Q21-559 | BD Bioscience | 563424 |
| Gata3 | BV711 | L50-823 | BD Bioscience | 565449 |
| **antibodies for human validation study** | | | | |
| CD14 | FITC | M5E2 | BD Bioscience | 555397 |
| CD16 b | APC/Fire 750 | V NK80 | BioLegend | 302060 |
| IL-1B | FITC | CRM56 | Invitrogen | 11-7018-42 |
| IL-8 | Pacific blue | E8N1 | BioLegend | 511420 |
| IL-18 | PE | 74801 | R&D Systems | IC646P |
| antibodies for mice | | | | |
| CD45 | AF700 | 30-F11 | BioLegend | 103128 |
| CD4 | PE-Cy5 | Gk1.5, | Invitrogen | 15004183 |
| CD4 | BV605 | RM4-5, | BioLegend | 100548 |
| CD8 | BV650 | 53-6.7 | BioLegend | 100742 |
| CD19 | BV711 | 6D5 | BioLegend | 115555 |
| Ly6C | PECy7 | AL-21 | BD Bioscience | 560593 |
| Ly6G | BV711 | 1A8 | BioLegend | 127643 |

| | | | | |
|---|---|---|---|---|
| CD25 | APC/Fire 750 | 3C7 | BioLegend | 101921 |
| CCR6 | BV421 | 29-2L17 | BioLegend | 129818 |
| CXCR3 | BV650 | CXCR3-173 | BioLegend | 126531 |
| VLA4 (CD49d) | AF647<br>BV786 | R1-2 | BD Bioscience | 564394<br>564397 |
| ICAM-1 | APC/Fire 750 | YN1/1.7.4 | BioLegend | 116126 |
| IL-11 | PE | 188520 | R&D Systems | MAB418 (custom labeled PE) |
| IL-10 | PerCpCy5.5 | JES5-16E3, | Invitrogen | 45-7101-82 |
| IL-23 | AF488 | c23cpg | Invitrogen | 53-7023-82 |
| IL-17 | BV510<br>BV605 | TC11-18H10.1<br>TC11-18H10 | BioLegend | 506933<br>64169 |
| GM-CSF | BV421 | MP1-22E9 | BD Bioscience | 564747 |
| IFN-γ | FITC | XMG1.2 | Invitrogen | 11-7311-82 |
| **antibodies for mouse validation study** | | | | |
| IL-1B | FITC | NJTEN3 | Invitrogen | 11-7114-82 |
| TLR7 | PE | A94B10 | BD Bioscience | 565557 |
| NLRP3 | APC | 768319 | R&D Systems | IC7578A |
| NFkB p65 | AF700 | 532301 | R&D Systems | IC5078N |
| antibodies for immunofluorescent staining | | | | |
| Rabbit anti-mouse CD4 | | ab183685 | Abcam | |
| Rabbit anti-rat Iba1 | | 019-19741 | Wako | |
| Rabbit anti-Myelin Basic Protein | | Ab40390 | Abcam | |
| Goat anti-Rat IgG Secondary Antibody | Cy3 | A10522 | Invitrogen | |
| Goat anti-Rabbit IgG Secondary Antibody | AF 488 | A-11008 | Invitrogen | |
| **primers for validation study in humans** | | | | |
| **Gene** | **Assay ID** | **supplier** | | |
| GAPDH | Hs02786624_g1 | ThermoFisher Scientific | | |
| NLRP3 | Hs00918082_m1 | ThermoFisher Scientific | | |
| NF-k β1 | Hs00765730_m1 | ThermoFisher Scientific | | |
| TLR4 | Hs00152939_m1 | ThermoFisher Scientific | | |
| PTGS2 (COX2) | Hs00153133_m1 | ThermoFisher Scientific | | |
| Caspase1 | Hs00354836_m1 | ThermoFisher Scientific | | |
| CXCL8 (IL-8) | Hs00174103_m1 | ThermoFisher Scientific | | |
| IL-18 | Hs01038788_m1 | ThermoFisher Scientific | | |
| IL-1 β | Hs01555410_m1 | ThermoFisher Scientific | | |
| IL-6 | Hs00174131_m1 | ThermoFisher Scientific | | |
| IL-1A | Hs00174092_m1 | ThermoFisher Scientific | | |
| IL-23 | Hs00372324_m1 | ThermoFisher Scientific | | |
| CXCL2 | Hs00601975_m1 | ThermoFisher Scientific | | |
| CCL3 | Hs00234142_m1 | ThermoFisher Scientific | | |
| CXCL3 | Hs00171061_m1 | ThermoFisher Scientific | | |
| CCL3L1 | Hs00824185_s1 | ThermoFisher Scientific | | |

| | | |
|---|---|---|
| MX1 | Hs00895608_m1 | ThermoFisher Scientific |
| CD81 | Hs01002167_m1 | ThermoFisher Scientific |
| CD99 | Hs00908455_m1 | ThermoFisher Scientific |
| IFITM3 | Hs03057129_s1 | ThermoFisher Scientific |
| VEGFB | Hs00173634_m1 | ThermoFisher Scientific |
| VEGFA | Hs00900055_m1 | ThermoFisher Scientific |
| C1QA | Hs00706358_s1 | ThermoFisher Scientific |
| C3 | Hs00163811_m1 | ThermoFisher Scientific |
| CXCL16 | Hs00222859_m1 | ThermoFisher Scientific |
| IFNGR1 | Hs00988304_m1 | ThermoFisher Scientific |
| IFI44 L | Hs00915292_m1 | ThermoFisher Scientific |
| IFI44 | Hs00197427_m1 | ThermoFisher Scientific |
| **primers for validation study in mice** | | |
| **Gene** | **Assay ID** | **supplier** |
| GAPDH | Mm99999915_g1 | ThermoFisher Scientific |
| NLRP3 | Mm00840904_m1 | ThermoFisher Scientific |
| NF-kβ1 | Mm00476361_m1 | ThermoFisher Scientific |
| CXCL3 | Hs00171061_m1 | ThermoFisher Scientific |
| VEGFa | Mm00437306_m1 | ThermoFisher Scientific |
| IL-1 β | Mm00434228_m1 | ThermoFisher Scientific |

**Legends for datasets:**

**Dataset S1.** Frequency and cell numbers, IL-11 vs. control

**Dataset S2.** DEGs in 29 clusters, IL-11 vs. control

**Dataset S3.** DEGs in IL-11 vs. control

**Dataset S4.** GO terms monocytes, IL-11 vs. control

**Dataset S5.** GO terms $CD4^+$ cells, IL-11 vs. control

**Dataset S6.** DEGs in 29 clusters, CSF vs. blood

**Dataset S7.** Frequency and cell numbers, CSF vs. blood

**Dataset S8.** DEGs in CSF vs. blood

**Dataset S9.** GO terms monocytes, CSF vs. blood.

## SI References:


1. A. J. Thompson *et al.*, Diagnosis of multiple sclerosis: 2017 revisions of the McDonald criteria. *Lancet Neurol* **17**, 162-173 (2018).

2. Y. Hao *et al.*, Integrated analysis of multimodal single-cell data. *Cell* (2021).

3. G. Monaco *et al.*, RNA-Seq signatures normalized by mRNA abundance allow absolute deconvolution of human immune cell types. *Cell reports* **26**, 1627-1640. e1627 (2019).

4. M. S. Seyedsadr *et al.*, Inactivation of sphingosine-1-phosphate receptor 2 (S1PR2) decreases demyelination and enhances remyelination in animal models of multiple sclerosis. *Neurobiology of Disease* **124**, 189-201 (2019).

5. X. Zhang *et al.*, IL-11 Induces Encephalitogenic Th17 Cells in Multiple Sclerosis and Experimental Autoimmune Encephalomyelitis. *J Immunol* **203**, 1142-1150 (2019).